

## Research Article

# A New Computational Technique for Analytic Treatment of Time-Fractional Nonlinear Equations Arising in Magneto-Acoustic Waves

D. G. Prakasha,<sup>1</sup> Rania Saadeh ,<sup>2</sup> Krunal Kachhia,<sup>3</sup> Ahmad Qazza ,<sup>2</sup> and Naveen Sanju Malagi <sup>1</sup>

<sup>1</sup>Department of Mathematics, Davangere University, Shivagangothri, Davangere 577007, India

<sup>2</sup>Department of Mathematics, Zarqa University, Zarqa 13110, Jordan

<sup>3</sup>Department of Mathematical Sciences, P. D. Patel Institute of Applied Sciences, Charotar University of Science and Technology, Changa, Anand 388421, Gujarat, India

Correspondence should be addressed to Ahmad Qazza; [aqazza@zu.edu.jo](mailto:aqazza@zu.edu.jo)

Received 8 December 2022; Revised 21 January 2023; Accepted 3 February 2023; Published 14 February 2023

Academic Editor: Amin Jajarmi

Copyright © 2023 D. G. Prakasha et al. This is an open access article distributed under the Creative Commons Attribution License, which permits unrestricted use, distribution, and reproduction in any medium, provided the original work is properly cited.

This paper presents the study of time-fractional nonlinear fifth-order Korteweg–de Vries equations by utilizing an adequate novel technique, namely, the  $q$ -homotopy analysis transform method. The fifth-order Korteweg–de Vries equation has got its importance in the study of magneto-sound propagation in plasma, capillary gravity water waves, and the motion of long waves under the influence of gravity in shallow water. To justify the effectiveness and pertinence of the contemplated technique, we take a look at three examples of the time-fractional fifth-order Korteweg–de Vries equations. The  $q$ -homotopy analysis transform method offers us to modulate the range of convergence of the series solution using  $h$ , called the auxiliary parameter or convergence control parameter. The study of the fractional behaviour of the considered equations expresses the originality of the presented work. There is a visible variation in the obtained solutions for different fractional orders and which can lead to different consequences for future work. As a future research direction, readers can use the hybrid methodologies merging with our projected scheme to achieve better consequences. Additionally, to validate the precision and reliability of the proposed method, we organized suitable numerical simulations. The obtained findings show that the proposed method is very gratifying and examines the complex nonlinear challenges that arise in science and innovation.

## 1. Introduction

As we can differentiate or integrate a function one time, two times, or any whole number of times, differentiation and integration both are treated as discrete mathematical operations. However, fractional order derivatives have adequate potential to tackle out most complex systems. The history of derivatives of fractional order was going back to the times of Leibnitz and L'Hospital. The concept of fractional calculus (FC) in the field of mathematical analysis is mainly focused on the scrutiny and application of integrals and derivatives of noninteger order. Indeed, this concept provides us with a great degree of freedom in solving various

types of equations (differential, integral, and integrodifferential), problems under mathematical physics involving some special functions and their generalizations, and extensions in one or more variables. Fractional calculus helps us to explain the naturalism of the universe in a brilliant and symmetric manner in the classical calculus. This is due to its ability to interpret the paradoxical attitude and memory effects that occur in nonlinear phenomena. The mathematical foundation for the concept of fractional order derivatives was excellently carried out with the efforts of pioneers such as Reimann [1], Podlubany [2], Liouville [3], Miller and Ross [4], Caputo [5], and many others. The speculation of fractional partial differential equations

captured consciousness, popularity, and importance by many mathematical minds during the past forty years and longer as the best way to make discoveries in science and engineering, particularly in chaos theory [6], human diseases [7, 8], fluid dynamics [9, 10], nanotechnology [11], financial models [12], biomathematics [13], and many others. To describe the tendency of nonlinear problems that exist in day-to-day life, the solutions of fractional differential equations play an essential role.

In physics, plasma is usually considered a distinct phase of matter and does not have a definite shape or volume. The plasma responds strongly to electromagnetic fields because the free electric charges make the plasma electrically conductive. Thus, making its properties dominated by electric and/or magnetic forces. The most significant pragmatic uses of plasmas lie in the field of intensity creation. Utilizing heat sources to convert water to steam, which powers turbo generators, has been a key approach for generating electric power. These heat sources depend on igniting petroleum derivatives such as oil, coal, and gaseous gasoline. In plasma, different types of acoustic waves will propagate and they are important for the heating mechanism. Compressible unsettling influences spread in plasma as magneto-acoustic waves driven by both gas pressure and attractive power. In part, ionized plasmas, the elements of ionized and unbiased species, are coupled because of particle nonpartisan impacts. As an outcome, the magneto-acoustic wave carries on as particle acoustic waves and Alfvén waves in the scope of the low magnetic field and low temperature, respectively. The magneto-acoustic waves have an important role in solar corona heating [10, 14].

The phenomenon of nonlinear equations describes the fundamental physical aspects in nature ranging from chaotic behaviour in biological systems [15], plasma physics-plasma containment in stellarators, and tokamaks to energy generation [16, 17], quantum mechanics [18], nonlinear optics [19], solid-state physics and up to fibre optical communication devices [20], dual wave soliton solution [21], unidirectional shallow water waves [22], analytical wave solutions [23], unmagnetized dust plasma [24], optimal solitons for the nonlinear dynamics [25], and so on [26–28]. The various phenomena of nonlinear equations are modelled in terms of many orders of nonlinear partial differential equations (29)–(31). Partial differential equations are largely utilised to represent physical systems, but unfortunately, many of them don't have the exact solution. Moreover, the accurate solution to this nonlinear phenomenon is not available in the literature and hence to solve these nonlinear systems, there is an essence of studying the nonlinear phenomena with appropriate and more efficient methods.

In 1895, two Dutch scientists, Korteweg and de Vries derived a celebrated generic model equipped with the nonlinear dispersive partial differential equation to study the motion of long waves with a smaller amplitude under the influence of gravity in shallow water, called Korteweg–de Vries (KdV) equation [32, 33]. Rayleigh's method of 1876 was elongated by Korteweg and de Vries to include the effect of capillarity, oscillatory waves, the study of higher-order

terms present in the Lagrange–Rayleigh expansion, and long waves of evolving shape.

Since the solution of the KdV equation can be explained exactly and precisely, it is predominantly distinguished as the archetypal illustration of an exactly solvable model [32, 34]. The KdV equation amalgamates dispersion and nonlinearity and provides stationary solutions tracing both periodic and solitary waves. This equation can be recast as follows:

$$u_t + cu_x + \alpha uu_x + \beta u_{xxx} = 0, \quad (1)$$

where  $c$ ,  $\alpha$ , and  $\beta$  are nonzero real parameters and  $u = u(x, t)$  is an unknown smooth function. Equation (1) represents a model for the interpretation of long waves which are weakly nonlinear with small dispersion in media. Here, if parameter  $c$  is zero, then the above equation includes a well-known evolution equation and the term  $u_t$  depicts the time evolution of the wave with the linear propagation in one direction. The nonlinear term  $u_x + \alpha uu_x$  deals for tilting of the wave, and the linear dispersive term  $u_{xxx}$  reports spreading of the wave. Subsequently, various kinds of KdV equations possess many remarkable properties and are being considered as a model to explain the wide range of physical phenomena which exist in the connected branches of mathematics and physics.

The fifth-order KdV equations are employed to investigate the numerous nonlinear dispersive phenomena in plasma waves when the third-order contributions are small. It has substantial usage in wave propagation [13] and can describe the real features in nonlinear optics and quantum physics. The general form of the fifth-order KdV equation is as follows:

$$u_t = u_{xxxxx} + f(x; t; u_x; u_{xx}; u_{xxx}). \quad (2)$$

There are various analytical and numerical methods available for handling various forms of fifth-order KdV-type equations in the literature. Some of them are the Adomian decomposition technique [35], modified Adomian decomposition method [36], Laplace decomposition approach [37], differential transform technique [38, 39], Hirota's bilinear techniques [40], inverse scattering algorithm [41], He's semi-inverse scheme [42], extended Tanh method [43], homotopy analysis technique [14, 44], fractional homotopy analysis transform algorithm [45], modified homotopy perturbation technique [46], variational iteration technique [47], homotopy perturbation method [48, 49], homotopy perturbation transform method [50], hyperbolic and exponential ansatz methods [51], multiple exp-function method [52], and others [53–55]. Moreover, many methods are available to solve the fractional-order KdV equations. In the present investigation, we consider the time-fractional fifth-order KdV equations with initial conditions as follows [56]:

$$D_t^\alpha u(x, t) + u_x + u^2 u_{xx} + u_x u_{xx} - 20u^2 u_{xxx} + u_{xxxxx} = 0, \quad (3)$$

with the initial condition  $u(x, 0) = 1/x$ .

$$D_t^\alpha u(x, t) + uu_x - uu_{xxx} + u_{xxxxx} = 0, \tag{4}$$

with initial conditions  $u(x, 0) = e^x$ .

$$D_t^\alpha u(x, t) + uu_x + u_{xxx} - u_{xxxxx} = 0, \tag{5}$$

with initial conditions  $u(x, 0) = 105/169 \operatorname{sech}^4(x - k/2\sqrt{13})$ .

Here, equations (3) and (4) are called fifth-order KdV equations and equation (5) is called the Kawahara equation.

KdV equations (3) and (4) are crucial for explaining how long waves move in shallow water when there is gravity. In order to study the propagation of oscillatory solitary waves in a dispersive medium, Kuwahara first applied Kawahara equation (5) in 1972 [57]. The above equations describe the interaction between nonlinearity and dispersion in the theoretically simplest terms possible. The higher-order nonlinear factors that are present in the equations under consideration express higher amplitude internal waves.

Now, the solutions for the abovementioned equations have been investigated by employing a new computational technique, known as the  $q$ -homotopy analysis transform method (or briefly,  $q$ -HATM). The considered technique is a graceful unification of the Laplace transform and homotopy algorithm [58]. Here, it is mentioned that Liao is the first person who introduced the concept of the homotopy analysis method [59, 60], which is an excellent analytical tool in order to get the solution of highly nonlinear problems that have physical parameters with small/large scale or not. The proposed technique gives a great degree of freedom in picking initial approximations and auxiliary linear operators; as a result, the complexity of the problem can be reduced by transforming it into an infinitely countable number of easier, linear subproblems, helping in reducing

the time of computational work. This method is an efficient delegacy to find numerical solutions to an enormous kind of physical problems existing in various fields of science, financial modelling, and engineering [61–64] and the references therein.

The article’s remaining portion is decorated as follows. The fundamental and standard definitions of the fractional derivatives, table of nomenclature, and also, the basic idea of Laplace transform of Caputo fractional derivative are presented in Section 2. The methodology of the considered analytical technique for nonlinear fractional partial differential equations can be seen in Section 3. The investigation of the considered problem along with the incorporation of their graphical results using the projected technique is shown in Section 4. Section 5 cites the description of the obtained results. Section 6 is decorated with the concluding remarks followed by the references.

## 2. Preliminaries

The fundamental formulations of fractional calculus and the Laplace transform, which are relevant in the current context, are provided in this portion of the article.

*Definition 1.* The fractional Riemann–Liouville integral of a function  $f(t) \in C_\mu (\mu \geq -1)$  is presented [2, 64] by the following formula:

$$J^\alpha f(t) = \frac{1}{\Gamma(\alpha)} \int_0^t (t - \vartheta)^{\alpha-1} f(\vartheta) d\vartheta. \tag{6}$$

*Definition 2.* The derivative of fractional order  $\alpha$  of  $f \in C_{-1}^n$  in the Liouville–Caputo sense is defined [5, 6] as follows:

$$D_t^\alpha f(t) = \begin{cases} \frac{d^n f(t)}{dt^n}, & \alpha = n \in \mathbb{N}, \\ \frac{1}{\Gamma(n - \alpha)} \int_0^t (t - \vartheta)^{n-\alpha-1} f^{(n)}(\vartheta) d\vartheta, & n - 1 < \alpha < n, n \in \mathbb{N}. \end{cases} \tag{7}$$

*Definition 3.* The Laplace transform (LT) of a Caputo fractional derivative  $D_t^\alpha f(t)$  is represented [6] as follows:

$$L[D_t^\alpha f(t)] = s^\alpha F(s) - \sum_{r=0}^{n-1} s^{\alpha-r-1} f^{(r)}(0^+), \quad (n - 1 < \alpha \leq n), \tag{8}$$

where  $F(s)$  is the representation of  $L[f(t)]$ .

## 3. The Basic Concept of the Q-HATM to Solve Nonlinear Fractional Partial Differential Equation (NFPDE)

To demonstrate the reliability of the considered technique, we will consider the NFPDE with the initial conditions as follows:

$$D_t^\alpha u(x, t) + Ru(x, t) + Nu(x, t) = f(x, t), \quad n - 1 < \alpha \leq n, \tag{9}$$

where  $D_t^\alpha u(x, t)$  symbolize noninteger order derivative of  $u(x, t)$  in the Liouville–Caputo sense,  $f(x, t)$  cites the source term, linear and nonlinear differential operators are represented by  $R$  and  $N$ , respectively.

Currently, putting the LT to equation (9) using Definition 3 leads to the following equation:

$$s^\alpha L[u(x, t)] - \sum_{k=0}^{n-1} s^{\alpha-k-1} u^{(k)}(x, 0) + L[Ru(x, t)] + L[Nu(x, t)] = L[f(x, t)]. \tag{10}$$

By simplifying equation (10), we have the following equation:

$$L[u(x, t)] - \frac{1}{s^\alpha} \sum_{k=0}^{n-1} s^{\alpha-k-1} u^k(x, 0) + \frac{1}{s^\alpha} (L[Ru(x, t)] + L[Nu(x, t)] - L[f(x, t)]) = 0, \tag{11}$$

where the nonlinear operator  $N$  is defined in complying with HAM lead to the following equation:

$$N[\varphi(x, t; q)] = L[\varphi(x, t; q)] - \frac{1}{s^\alpha} \sum_{k=0}^{n-1} s^{\alpha-k-1} \varphi^{(k)}(x, t; q)(0^+) + \frac{1}{s^\alpha} \{L[R\varphi(x, t; q)] + L[N\varphi(x, t; q)] - L[f(x, t)]\}, \tag{12}$$

where  $\varphi(x, t; q)$  is a real function of  $x, t$  and  $q$  and  $q \in [0, 1/n]$ .

The zero<sup>th</sup> order deformation equation involving the auxiliary function  $H(x, t)$  is as follows:

$$(1 - nq)L[\varphi(x, t; q) - u_0(x, t)] = \hbar q H(x, t) N[\varphi(x, t; q)], \tag{13}$$

where  $\hbar \neq 0$  is the convergence control parameter,  $L$  symbolizes the Laplace transform,  $q \in [0, 1/n]$  ( $n \geq 1$ ) is the embedding parameter,  $u_0(x, t)$  is an initial guess of  $u(x, t)$ ,  $\varphi(x, t; q)$  is an unknown function. The following equations justify for  $q = 0$  and  $q = 1/n$ :

$$\varphi(x, t; 0) = u_0(x, t), \varphi\left(x, t; \frac{1}{n}\right) = u(x, t), \tag{14}$$

respectively. As we move  $q$  from 0 to  $1/n$ , the solution  $\varphi(x, t; q)$  converges from  $u_0(x, t)$  to the solution  $u(x, t)$ . After operating, the Taylor theorem for the function  $\varphi(x, t; q)$  around  $q$  leads to the following equation:

$$\varphi(x, t; q) = u_0(x, t) + \sum_{m=1}^{\infty} u_m(x, t) q^m, \tag{15}$$

where

$$u_m(x, t) = \frac{1}{m!} \frac{\partial^m \varphi(x, t; q)}{\partial q^m} \Big|_{q=0}. \tag{16}$$

On choosing the appropriate auxiliary parameter  $\hbar$ , the initial guess  $u_0(x, t)$ , and  $H(x, t)$ , the auxiliary linear operator, series (15) converges at  $q = 1/n$ , which leads to one of the solutions of the original nonlinear equation as follows:

$$u(x, t) = u_0(x, t) + \sum_{m=1}^{\infty} u_m(x, t) \left(\frac{1}{n}\right)^m. \tag{17}$$

Next, the  $m^{\text{th}}$  order deformation equation obtained by differentiating the zeroth order deformation equation  $m$ -times followed by dividing the resulting equation by  $m!$  at  $q = 0$  leads to the following equation:

$$L[u_m(x, t) - K_m u_{m-1}(x, t)] = \hbar H(x, t) \mathfrak{R}_m(\vec{u}_{m-1}), \tag{18}$$

and the vector  $\vec{u}_m$  is demarcated as follows:

$$\vec{u}_m = \{u_0(x, t), u_1(x, t), \dots, u_m(x, t)\}. \tag{19}$$

The following recursive is obtained by hiring the inverse Laplace transform to equation (18) as follows:

$$u_m(x, t) = K_m u_{m-1}(x, t) + \hbar L^{-1} [H(x, t) \mathfrak{R}_m(\vec{u}_{m-1})], \tag{20}$$

where

$$\mathfrak{R}_m(\vec{u}_{m-1}) = \frac{1}{(m-1)!} \frac{\partial^{m-1} N[\varphi(x, t; q)]}{\partial q^{m-1}} \Big|_{q=0}. \tag{21}$$

$$K_m = \begin{cases} 0, & m \leq 1, \\ n, & m > 1. \end{cases} \tag{22}$$

Lastly, the terms of the  $q$ -HATM series solution are attained by evaluating equation (20).

#### 4. Application of the Considered Scheme to Solve the Nonlinear Time-Fractional Fifth-Order KdV Equation

The investigation of the following examples witnesses the efficacy and resolution of the contemplated scheme.

*Example 1.* The fifth-order time-fractional KdV equation defined in equation (3) is as follows:

$$D_t^\alpha u(x, t) + u_x + u^2 u_{xx} + u_x u_{xx} - 20u^2 u_{xxx} + u_{xxxxx} = 0, \tag{23}$$

with the initial condition

$$u(x, 0) = \frac{1}{x}. \tag{24}$$

We introduced LT in equation (23) along with the starting solution in equation (24), which leads to the following equation:

$$L[u(x, t)] - \frac{1}{s} \left\{ \frac{1}{x} \right\} + \frac{1}{s^\alpha} L \left\{ \frac{\partial u}{\partial x} + u^2 \frac{\partial^2 u}{\partial x^2} + \frac{\partial u}{\partial x} \frac{\partial^2 u}{\partial x^2} - 20u^2 \frac{\partial^3 u}{\partial x^3} + \frac{\partial^5 u}{\partial x^5} \right\} = 0. \tag{25}$$

The nonlinear operator  $N$  is defined as follows:

$$N[\varphi(x, t; q)] = L[\varphi(x, t; q)] - \frac{1}{s} \left\{ \frac{1}{x} \right\} + \frac{1}{s^\alpha} L \left\{ \frac{\partial \varphi(x, t; q)}{\partial x} + \varphi^2(x, t; q) \frac{\partial^2 \varphi(x, t; q)}{\partial x^2} + \frac{\partial \varphi(x, t; q)}{\partial x} \frac{\partial^2 \varphi(x, t; q)}{\partial x^2} - 20\varphi^2(x, t; q) \frac{\partial^3 \varphi(x, t; q)}{\partial x^3} + \frac{\partial^5 \varphi(x, t; q)}{\partial x^5} \right\}. \tag{26}$$

The  $m^{\text{th}}$  order deformation equation is as follows:

$$L[u_m(x, t) - K_m u_{m-1}(x, t)] = \hbar \mathfrak{R}_m[\vec{u}_{m-1}], \tag{27}$$

where

$$\mathfrak{R}_m[\vec{u}_{m-1}] = L[u(x, t)] - \left(1 - \frac{K_m}{n}\right) \frac{1}{s} \left\{ \frac{1}{x} \right\} + \frac{1}{s^\alpha} L \left\{ \frac{\partial u_{m-1}}{\partial x} + \sum_{j=0}^i \sum_{i=0}^{m-1} u_j u_{i-j} \frac{\partial^2 u_{m-1-i}}{\partial x^2} + \sum_{i=0}^{m-1} \frac{\partial u_i}{\partial x} \frac{\partial^2 u_{m-1-i}}{\partial x^2} - 20 \sum_{j=0}^i \sum_{i=0}^{m-1} u_j u_{i-j} \frac{\partial^3 u_{m-1-i}}{\partial x^3} + \frac{\partial^5 u_{m-1}}{\partial x^5} \right\}. \tag{28}$$

On implementing inverse LT with equation (27), we get the following equation:

$$u_m(x, t) = K_m u_{m-1}(x, t) + \hbar L^{-1} \left\{ \mathfrak{R}_m[\vec{u}_{m-1}] \right\}. \tag{29}$$

Solving the above equations consistently gives the following equation:

$$\begin{aligned} u_0(x, t) &= \frac{1}{x}, \\ u_1(x, t) &= \frac{\hbar t^\alpha}{\Gamma[\alpha + 1]} \left( -\frac{1}{x^2} \right), \\ u_2(x, t) &= \frac{(n + \hbar)\hbar t^\alpha}{\Gamma[\alpha + 1]} \left( -\frac{1}{x^2} \right) + \frac{2t^{2\alpha}\hbar^2}{x^3\Gamma[2\alpha + 1]}, \\ u_3(x, t) &= \frac{(n + \hbar)^2\hbar t^\alpha}{\Gamma[\alpha + 1]} \left( -\frac{1}{x^2} \right) + \frac{2(n + \hbar)t^{2\alpha}\hbar^2}{x^3\Gamma[2\alpha + 1]} - \frac{2t^{3\alpha}\hbar^3 \left( (1080 + 2x + 3x^4)\Gamma[1 + \alpha]^2 - (540 + x)\Gamma[2\alpha + 1] \right)}{x^8\Gamma[\alpha + 1]^2\Gamma[3\alpha + 1]}, \\ &\vdots \end{aligned} \tag{30}$$

Finally, after getting further iterative terms, the essential series solution of equation (23) is presented by the following equation:

$$u(x, t) = u_0(x, t) + \sum_{m=1}^{\infty} u_m(x, t) \left( \frac{1}{n} \right)^m. \tag{31}$$

By taking  $\alpha = 1, \hbar = -1,$  and  $n = 1,$  then the obtained solution  $\sum_{m=1}^N u_m(x, t) (1/n)^m$  converges to the exact solution  $u(x, t) = 1/x - t$  of equation (23), as  $N \rightarrow \infty.$

*Example 2.* Consider the nonlinear time-fractional fifth-order KdV equation cited in equation (4) as follows:

$$D_t^\alpha u(x, t) + uu_x - uu_{xxx} + u_{xxxxx} = 0, \tag{32}$$

with initial conditions

$$u(x, 0) = e^x. \tag{33}$$

We introduced LT in equation (32) along with the starting solution in equation (33), which leads to the following equation:

$$L[u(x, t)] - \frac{e^x}{s} + \frac{1}{s^\alpha} L \left\{ u \frac{\partial u}{\partial x} - u \frac{\partial^3 u}{\partial x^3} + \frac{\partial^5 u}{\partial x^5} \right\} = 0. \tag{34}$$

The nonlinear operator  $N$  is defined as follows:

$$N[\varphi(x, t; q)] = L[\varphi(x, t; q)] - \frac{e^x}{s} + \frac{1}{s^\alpha} L \left\{ \varphi(x, t; q) \frac{\partial \varphi(x, t; q)}{\partial x} - \varphi(x, t; q) \frac{\partial^3 \varphi(x, t; q)}{\partial x^3} + \frac{\partial^5 \varphi(x, t; q)}{\partial x^5} \right\}. \tag{35}$$

The  $m^{\text{th}}$  order deformation equation is as follows:

$$L[u_m(x, t) - K_m u_{m-1}(x, t)] = \hbar \mathfrak{R}_m [\vec{u}_{m-1}], \tag{36}$$

where

$$\mathfrak{R}_m [\vec{u}_{m-1}] = L[u(x, t)] - \left(1 - \frac{K_m}{n}\right) \left\{ \frac{e^x}{s} \right\} + \frac{1}{s^\alpha} L \left\{ \sum_{i=0}^{m-1} u_i \frac{\partial u_{m-1-i}}{\partial x} - \sum_{i=0}^{m-1} u_i \frac{\partial^3 u_{m-1-i}}{\partial x^3} + \frac{\partial^5 u_{m-1}}{\partial x^5} \right\}. \tag{37}$$

When treated with inverse LT with equation (36), we get the following equation:

$$u_m(x, t) = K_m u(x, t) + \hbar L^{-1} \{ \mathfrak{R}_m [\vec{u}_{m-1}] \}. \tag{38}$$

Solving the above equations consistently gives the following equation:

$$\begin{aligned} u_0(x, t) &= e^x, \\ u_1(x, t) &= \frac{\hbar t^\alpha e^x}{\Gamma[\alpha + 1]}, \\ u_2(x, t) &= \frac{(n + \hbar) \hbar t^\alpha e^x}{\Gamma[\alpha + 1]} + \frac{[ee]^x t^{2\alpha} \hbar^2}{\Gamma[2\alpha + 1]}, \\ u_3(x, t) &= \frac{(n + \hbar)^2 \hbar t^\alpha e^x}{\Gamma[\alpha + 1]} + \frac{(n + \hbar) [ee]^x t^{2\alpha} \hbar^2}{\Gamma[2\alpha + 1]} + \frac{[ee]^x t^{3\alpha} \hbar^3}{\Gamma[3\alpha + 1]}, \\ &\vdots \end{aligned} \tag{39}$$

Finally, after getting further iterative terms, the essential series solution of equation (32) is presented by the following equation:

$$u(x, t) = u_0(x, t) + \sum_{m=1}^{\infty} u_m(x, t) \left(\frac{1}{n}\right)^m. \tag{40}$$

Taking  $n = 1$ ,  $\hbar = -1$ , and  $\alpha = 1$ , then the solution which we obtained is in the form  $\sum_{m=1}^N u_m(x, t) (1/n)^m$  that converges to the exact solution  $u(x, t) = e^{x-t}$  of equation (31), equation as  $N \rightarrow \infty$ .

*Example 3.* We considered the time-fractional fifth-order KdV equation considered in equation (5) as follows:

$$D_t^\alpha u(x, t) + uu_x + u_{xxx} - u_{xxxxx} = 0, \tag{41}$$

with initial condition

$$u(x, 0) = \frac{105}{169} \operatorname{sech}^4 \left( \frac{x-k}{2\sqrt{13}} \right). \tag{42}$$

By performing Laplace transform on equation (41) and then considering equation (42), we get the following equation:

$$L[u(x, t)] - \frac{1}{s} \left( \frac{105}{169} \operatorname{sech}^4 \left( \frac{x-k}{2\sqrt{13}} \right) \right) + \frac{1}{s^\alpha} L \left\{ u \frac{\partial u}{\partial x} + \frac{\partial^3 u}{\partial x^3} - \frac{\partial^5 u}{\partial x^5} \right\} = 0. \quad (43)$$

The nonlinear operator  $N$  is defined as follows:

$$N[\varphi(x, t; q)] = L[\varphi(x, t; q)] - \frac{1}{s} \left\{ \frac{105}{169} \operatorname{sech}^4 \left( \frac{x-k}{2\sqrt{13}} \right) \right\} + \frac{1}{s^\alpha} L \left\{ \varphi(x, t; q) \frac{\partial \varphi(x, t; q)}{\partial x} + \frac{\partial^3 \varphi(x, t; q)}{\partial x^3} - \frac{\partial^5 \varphi(x, t; q)}{\partial x^5} \right\}. \quad (44)$$

The  $m^{\text{th}}$  order deformation equation is as follows: where

$$L[u_m(x, t) - K_m u_{m-1}(x, t)] = \hbar \mathfrak{R}_m [\vec{u}_{m-1}], \quad (45)$$

$$\mathfrak{R}_m [\vec{u}_{m-1}] = L[u(x, t)] - \left( 1 - \frac{K_m}{n} \right) \frac{1}{s} \left\{ \frac{105}{169} \operatorname{sech}^4 \left( \frac{x-k}{2\sqrt{13}} \right) \right\} + \frac{1}{s^\alpha} L \left\{ \sum_{i=0}^{m-1} u_i \frac{\partial u_{m-1-i}}{\partial x} + \frac{\partial^3 u_{m-1-i}}{\partial x^3} - \frac{\partial^5 u_{m-1-i}}{\partial x^5} \right\}. \quad (46)$$

By enforcing the inverse LT with equation (45), we get the following equation:

$$u_m(x, t) = K_m u(x, t) + \hbar L^{-1} \left\{ \mathfrak{R}_m [\vec{u}_{m-1}] \right\}. \quad (47)$$

Solving the above equations consistently gives the following equation:

$$\begin{aligned} u_0(x, t) &= \frac{105}{169} \operatorname{sech}^4 \left( \frac{x-k}{2\sqrt{13}} \right), \\ u_1(x, t) &= -\frac{7560 \hbar t^\alpha}{28561 \sqrt{13} \Gamma[\alpha+1]} \operatorname{sech}^4 \left( \frac{x-k}{2\sqrt{13}} \right) \tanh \left( \frac{x-k}{2\sqrt{13}} \right), \\ u_2(x, t) &= -\frac{(n+\hbar)7560 \hbar t^\alpha}{28561 \sqrt{13} \Gamma[\alpha+1]} \operatorname{sech}^4 \left( \frac{x-k}{2\sqrt{13}} \right) \tanh \left( \frac{x-k}{2\sqrt{13}} \right) \\ &\quad + \frac{136080 t^{2\alpha} \hbar^2 \operatorname{sech}^6 \left( \frac{x-k}{2\sqrt{13}} \right)}{62748517 \Gamma[1+2\alpha]} \left( -3 + 2 \cosh \left( \frac{x-k}{\sqrt{13}} \right) \right), \\ u_3(x, t) &= -\frac{7560(n+\hbar)^2 \hbar t^\alpha}{28561 \sqrt{13} \Gamma[\alpha+1]} \operatorname{sech}^4 \left( \frac{x-k}{2\sqrt{13}} \right) \tanh \left( \frac{x-k}{2\sqrt{13}} \right) + \frac{(n+\hbar)136080 t^{2\alpha} \hbar^2 \operatorname{sech}^6 \left( \frac{x-k}{2\sqrt{13}} \right)}{62748517 \Gamma[2\alpha+1]} \left( -3 + 2 \cosh \left( \frac{x-k}{\sqrt{13}} \right) \right) \\ &\quad + \frac{204120 t^{3\alpha} \hbar^3}{10604499373 \sqrt{13} \Gamma[1+\alpha]^2 \Gamma[1+3\alpha]} \operatorname{sech}^{10} \left( \frac{x-k}{2\sqrt{13}} \right) \tanh \left( \frac{x-k}{2\sqrt{13}} \right) \tanh \left( \frac{x-k}{2\sqrt{13}} \right) \times \\ &\quad \left( \left( -765 + 650 \cosh \left( \frac{x-k}{\sqrt{13}} \right) \right) + 9 \cosh \left( \frac{2(x-k)}{\sqrt{13}} \right) \Gamma[1+\alpha]^2 - 6 \cosh \left( \frac{3(x-k)}{\sqrt{13}} \right) \right) \Gamma[1+\alpha]^2 \\ &\quad + 140 \left( 3 - 2 \cosh \left( \frac{x-k}{\sqrt{13}} \right) \right) \Gamma[1+2\alpha], \end{aligned}$$

⋮

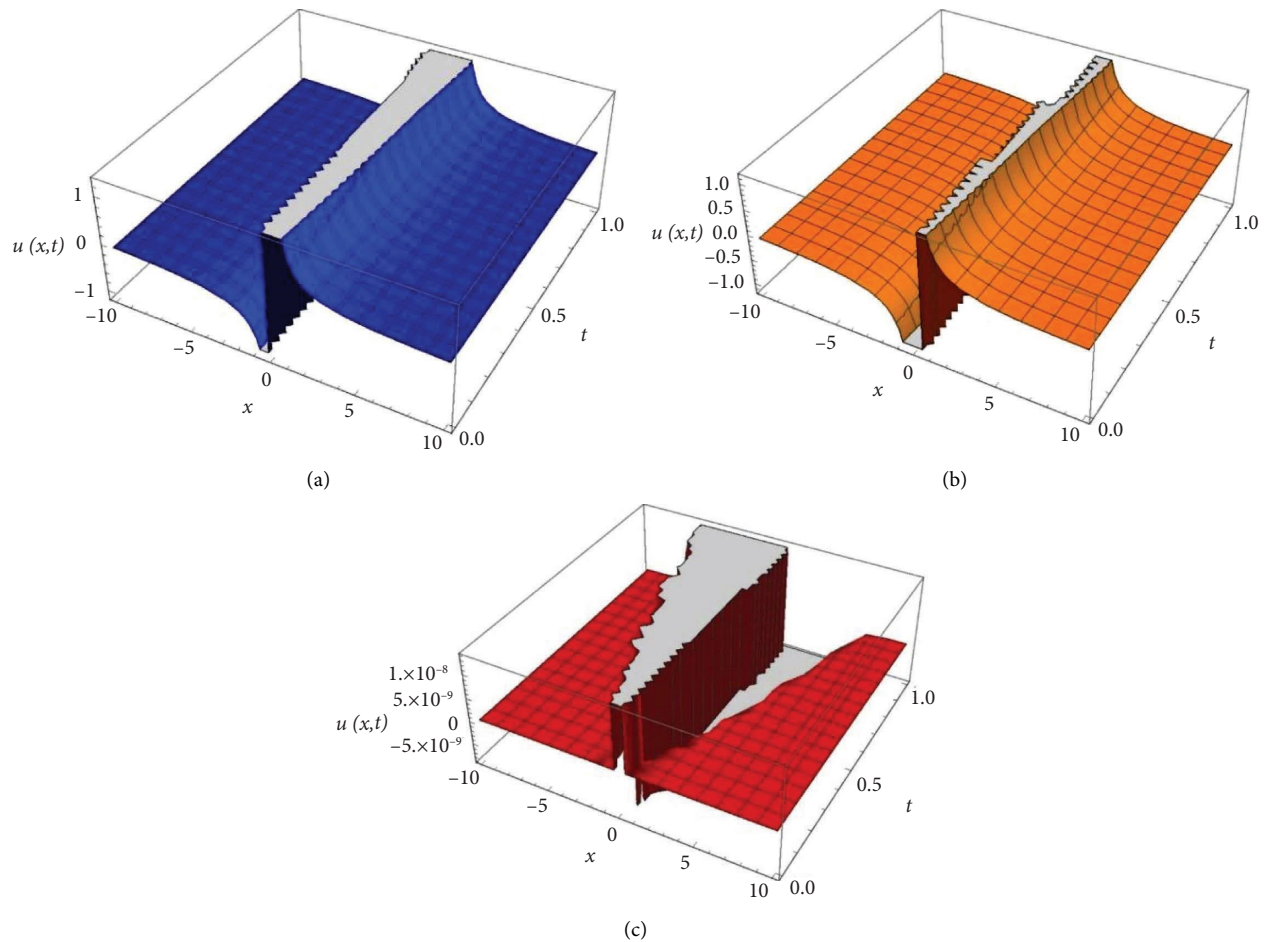


FIGURE 1: (a) 3D plot for the  $q$ -HATM solution, (b) surface of the exact solution, and (c) approximated solution surface at  $\alpha = 1$ ,  $n = 1$ , and  $\hbar = -1$  for Example 1.

Finally, after getting further iterative terms, the essential series solution of equation (41) is presented by the following equation:

$$u(x, t) = u_0(x, t) + \sum_{m=1}^{\infty} u_m(x, t) \left(\frac{1}{n}\right)^m. \quad (49)$$

If we take  $\hbar = -1$ ,  $\alpha = 1$ , and  $n = 1$ , then the secured solution  $\sum_{m=1}^N u_m(x, t) (1/n)^m$  converges to the exact solution  $u(x, t) = 105/169 \operatorname{sech}^4(1/2\sqrt{13}(x + 36t/169 - k))$  of equation (41) as  $N \rightarrow \infty$ .

## 5. Numerical Results and Discussion

This portion of the article provides incorporation of numerical simulations of the investigated problem that show the validity and effectiveness of the considered scheme  $q$ -HATM. Moreover, we incorporated a detailed description of the graphical solutions that were found. The secured results are very satisfying and in good fit with the exact solutions to the contemplated problem. The comparison of 3D surface plots of the obtained approximate solution and the exact solution along with their absolute error solutions is presented in Figure 1. We can see the accuracy of the obtained

approximated solution of Example 1 in Figure 1(c) with the least error values. The nature of the obtained solutions for different fractional order  $\alpha$  as we move along time  $t$  is cited in Figure 2. We can see the variation in the solution affected by different fractional orders. Figure 3 cites the plot of solution curves for distinct fractional orders, which gives the precise range of convergence control parameter  $\hbar$  to achieve convergence. The figure shows that we can choose  $\hbar$  values between  $-1.4$  and  $-0.4$  for the faster convergence of the approximated solution towards the exact solution. The convergence of the obtained solution is achieved by considering  $\hbar = -1$  in this work. Table 1 depicts the comparison of secured results with the homotopy perturbation transform method (HPTM) in terms of absolute error values with  $\hbar = -1$ ,  $n = 1$ , and  $\alpha = 1$ . The calculations of Table 1 are carried out by taking  $x = -6, 6$ , and  $8$  with the time interval  $[0, 0.5]$ . Surface plots of the  $q$ -HATM solution, the exact solution, and the approximated error solution for Example 2 are cited in Figure 4. The 2D plot of the obtained solution of Example 2 with respect to time  $t$  for different fractional order  $\alpha$  is cited in Figure 5. We can observe that the solution curve leads to different consequences for different fractional orders  $\alpha$ . The performance of  $n$  with  $\hbar$  in an accomplished outcome of the provided method is shown in Figure 6. The solution of



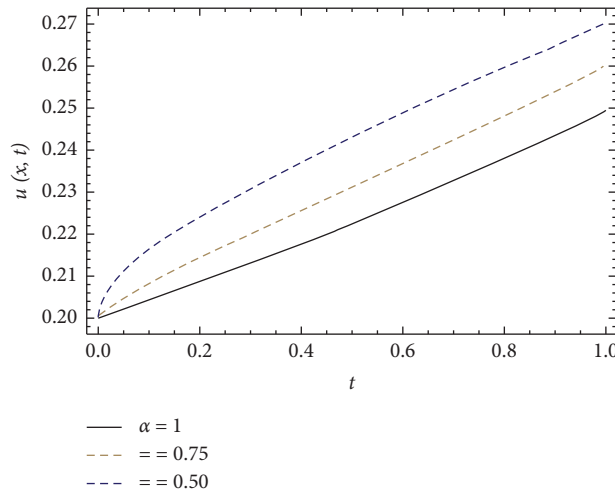


FIGURE 2:  $u(x, t)$  versus  $t$  for contemplated Example 1 when  $\hbar = -1, x = 5$ , and  $n = 1$  for distinct  $\alpha$ .

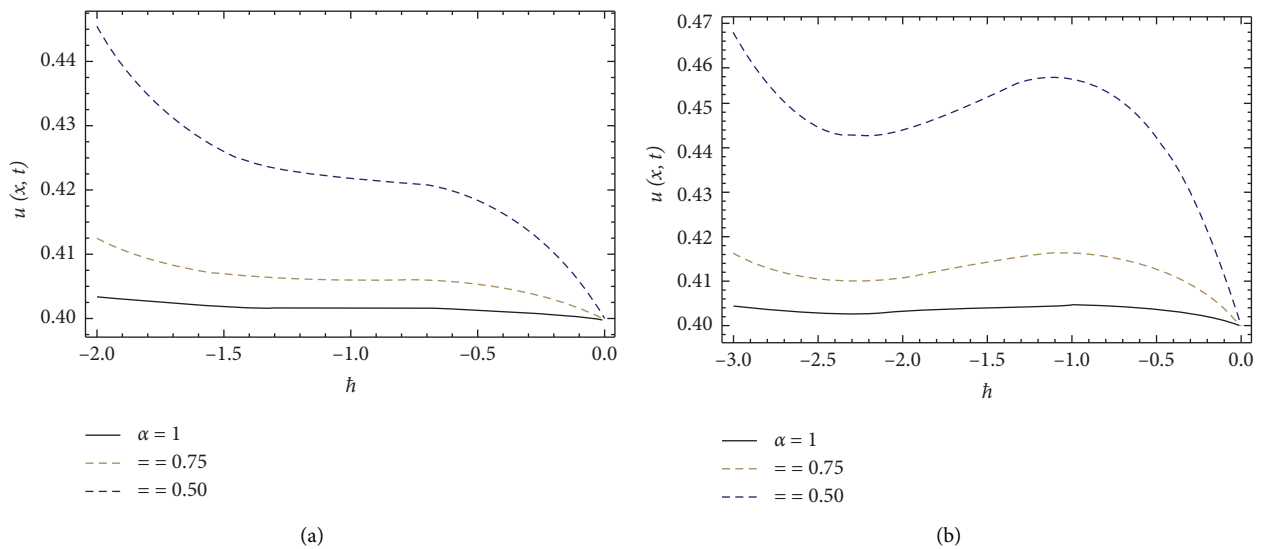


FIGURE 3:  $\hbar$ -curve for the acquired solution  $y(x, t)$  versus  $\hbar$  for considered Example 1 when (a)  $n = 1$  and (b)  $n = 2$  when  $t = 0.01, x = 2.5$  for distinct  $\alpha$ .

TABLE 1: Comparison of secured 3<sup>rd</sup> and 6<sup>th</sup>-order  $q$ -HATM solutions with HPTM [14] in terms of absolute error values for Example 1 at  $\hbar = -1, \alpha = 1$ , and  $n = 1$ .

$x$	$t$	$u_{\text{HPTM}}^{(3)}(x, t)$ [14]	$u_{q\text{-HATM}}^{(3)}(x, t)$	$u_{\text{HPTM}}^{(6)}(x, t)$ [15]	$u_{q\text{-HATM}}^{(6)}(x, t)$
-6	0	0	0	0	0
	0.1	$1.01250 \times 10^{-8}$	$1.26493 \times 10^{-8}$	$2.00000 \times 10^{-12}$	$5.85415 \times 10^{-14}$
	0.2	$1.58853 \times 10^{-7}$	$1.99124 \times 10^{-7}$	$8.00000 \times 10^{-12}$	$7.37493 \times 10^{-12}$
	0.3	$7.88790 \times 10^{-7}$	$9.92063 \times 10^{-7}$	$1.0300 \times 10^{-10}$	$1.24008 \times 10^{-10}$
	0.4	$2.44582 \times 10^{-6}$	$3.08642 \times 10^{-6}$	$7.66000 \times 10^{-10}$	$9.14495 \times 10^{-10}$
	0.5	$5.85975 \times 10^{-7}$	$7.41928 \times 10^{-6}$	$3.61500 \times 10^{-9}$	$4.29356 \times 10^{-9}$
6	0	0	0	0	0
	0.1	$1.43062 \times 10^{-6}$	$1.30780 \times 10^{-8}$	$1.41911 \times 10^{-6}$	$6.05531 \times 10^{-14}$
	0.2	$5.64584 \times 10^{-6}$	$2.12857 \times 10^{-7}$	$5.55361 \times 10^{-6}$	$7.88358 \times 10^{-12}$
	0.3	$1.25341 \times 10^{-5}$	$1.09649 \times 10^{-6}$	$1.22222 \times 10^{-5}$	$1.37061 \times 10^{-10}$
	0.4	$2.19832 \times 10^{-5}$	$3.52734 \times 10^{-6}$	$2.12426 \times 10^{-5}$	$1.04514 \times 10^{-9}$
	0.5	$3.38845 \times 10^{-5}$	$8.76824 \times 10^{-6}$	$3.24352 \times 10^{-5}$	$5.07421 \times 10^{-9}$

TABLE 1: Continued.

$x$	$t$	$u_{\text{HPTM}}^{(3)}(x, t)$ [14]	$u_{q\text{-HATM}}^{(3)}(x, t)$	$u_{\text{HPTM}}^{(6)}(x, t)$ [15]	$u_{q\text{-HATM}}^{(6)}(x, t)$
	0	0	0	0	0
8	0.1	$3.10937 \times 10^{-9}$	$3.09039 \times 10^{-9}$	$1.89934 \times 10^{-12}$	$6.02791 \times 10^{-15}$
	0.2	$5.00750 \times 10^{-8}$	$5.00801 \times 10^{-8}$	$4.34135 \times 10^{-11}$	$7.8252 \times 10^{-13}$
	0.3	$2.56853 \times 10^{-7}$	$2.56823 \times 10^{-7}$	$4.34570 \times 10^{-11}$	$1.35434 \times 10^{-11}$
	0.4	$8.22400 \times 10^{-7}$	$8.22368 \times 10^{-7}$	$1.34375 \times 10^{-10}$	$1.02796 \times 10^{-10}$
	0.5	$2.03447 \times 10^{-6}$	$2.03451 \times 10^{-6}$	$4.63377 \times 10^{-10}$	$4.96705 \times 10^{-10}$

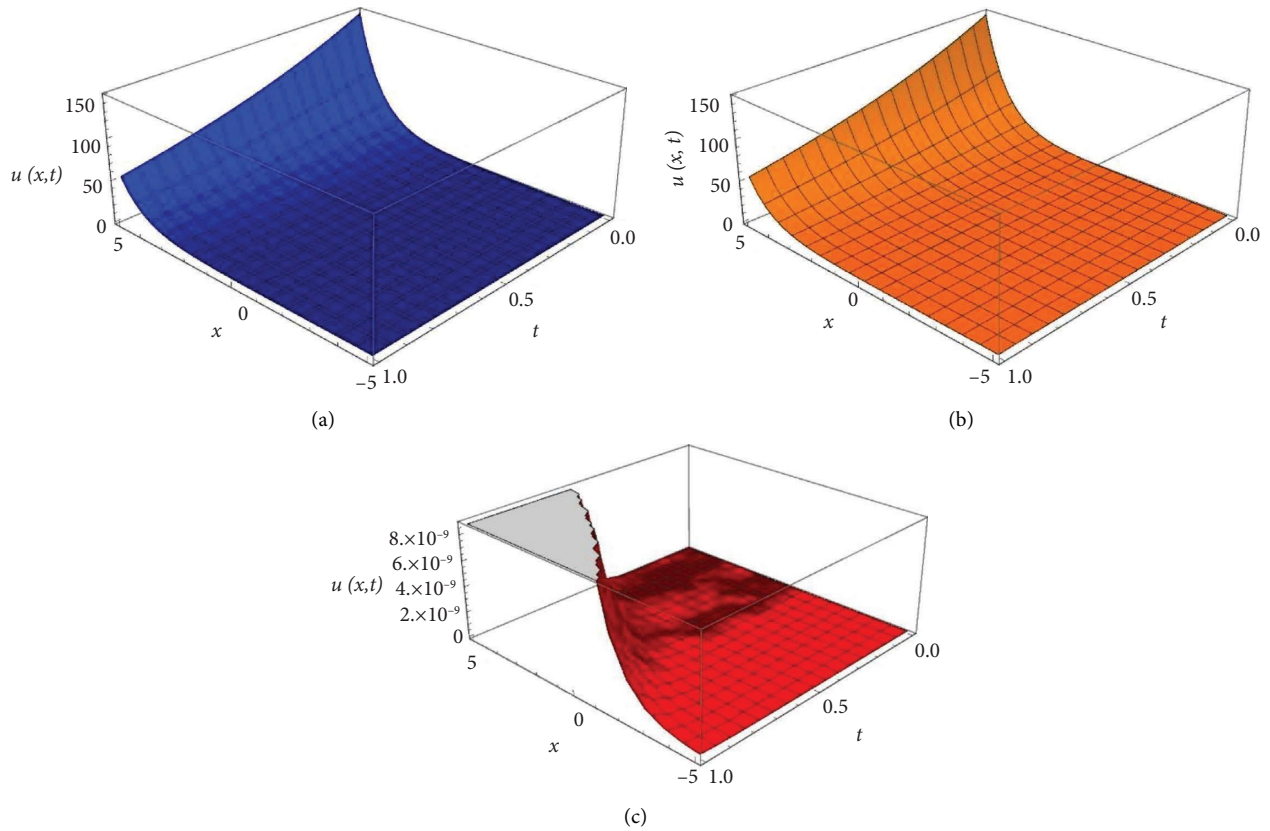


FIGURE 4: 3D plots of solution surfaces indicating  $q$ -HATM solution, the exact solution, and an approximated error solution, respectively (a-c) at  $\alpha = 1, n = 1$ , and  $\hbar = -1$  for Example 2.

Example 2 in terms of an absolute error from 3<sup>rd</sup>-order to 6<sup>th</sup>-order approximations is given in Table 2. That shows we can achieve better results by increasing the number of iterations. Figures 7(a) and 7(b) explore the 3D surfaces of the  $q$ -HATM solution and the exact solution of Example 3. The approximated absolute error solution of Example 3 is cited in Figure 7(c). The fractional behaviour of the considered nonlinear time-fractional fifth-order KdV equation over time  $t$  for distinct fractional order  $\alpha$  is plotted in Figure 8. To attain the precise range of convergence control parameters to have a faster rate of convergence to the exact solution, we have plotted Figure 9. Table 3 cites the approximated absolute error values of Example 4.3 for different values of  $x$  and  $t$ .

The 3D plots presented in Figures 1, 4, and 7 describe the wavy nature of the considered nonlinear KdV equations. For the purpose of accuracy we can consider the plots for the fractional/classical order  $\alpha = 1$ , there we can see the close association of the  $q$ -HATM solution with the exact solution. The physical interpretation of the considered fractional problems is well described by the fractional orders  $\alpha = 0.75$  and  $\alpha = 0.50$  due to their feature of memory effect. From the 2D plots, one can see the considered value for the convergence control parameter  $\hbar = -1$  works for all the fractional orders.

From all figures, we can observe that the hired fractional operator in the considered model exemplifies some interesting consequences and it authorizes the model which

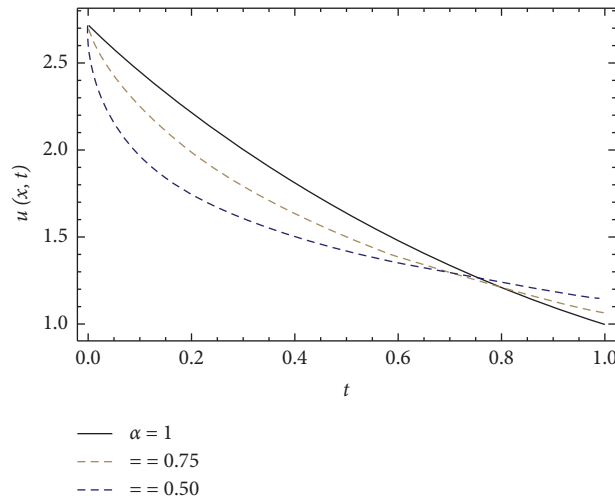


FIGURE 5:  $u(x, t)$  versus  $t$  for the contemplated Example 2 at  $\hbar = -1, x = 5$ , and  $n = 1$  for distinct of  $\alpha$ .

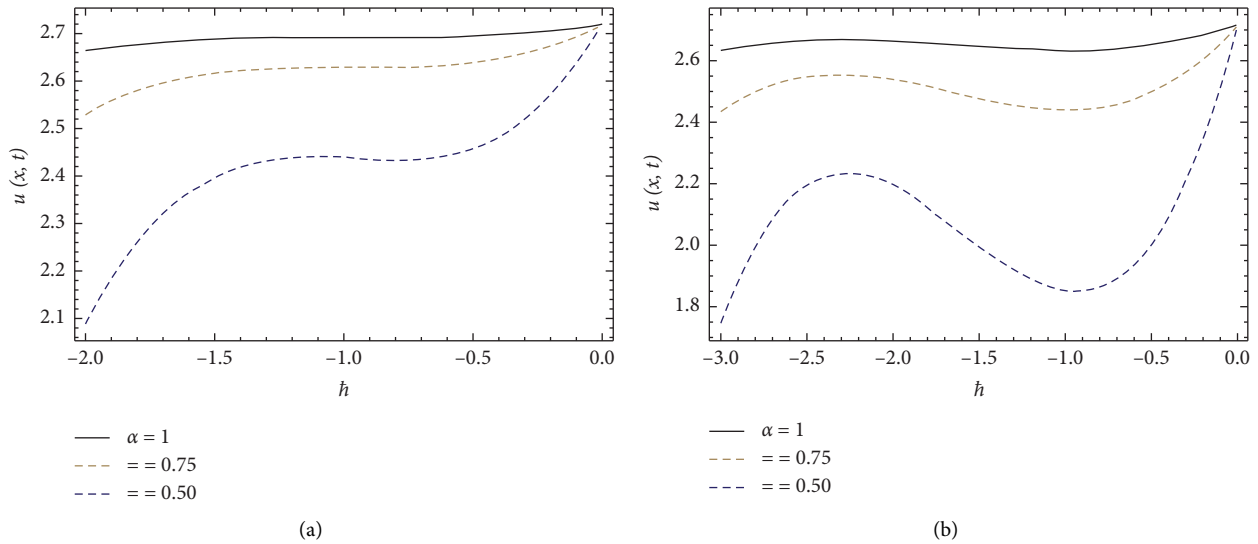


FIGURE 6:  $h$ -curve for acquired solution  $u(x, t)$  for Example 2 when (a)  $n = 1$  and (b)  $n = 2$  when  $x = 1$  and  $t = 0.001$  for distinct  $\alpha$ .

TABLE 2: This cites the 3<sup>rd</sup> to 6<sup>th</sup>-order approximations of the obtained q-HATM series solution for Example 2 at  $\hbar = -1, \alpha = 1$ , and  $n = 1$ .

$x$	$t$	$u_{q\text{-HATM}}^{(3)}(x, t)$	$u_{q\text{-HATM}}^{(4)}(x, t)$	$u_{q\text{-HATM}}^{(5)}(x, t)$	$u_{q\text{-HATM}}^{(6)}(x, t)$
-5	0	0	0	0	0
	0.1	$2.75225 \times 10^{-8}$	$5.52269 \times 10^{-10}$	$9.22623 \times 10^{-12}$	$1.32034 \times 10^{-13}$
	0.2	$4.31811 \times 10^{-7}$	$1.73856 \times 10^{-8}$	$5.82235 \times 10^{-10}$	$1.66938 \times 10^{-11}$
	0.3	$2.14415 \times 10^{-6}$	$1.29903 \times 10^{-7}$	$6.54040 \times 10^{-9}$	$2.81769 \times 10^{-10}$
	0.4	$6.64842 \times 10^{-6}$	$5.38726 \times 10^{-7}$	$3.62459 \times 10^{-8}$	$2.08553 \times 10^{-9}$
	0.5	$1.59285 \times 10^{-5}$	$1.61828 \times 10^{-6}$	$1.36397 \times 10^{-7}$	$9.82624 \times 10^{-9}$
5	0	0	0	0	0
	0.1	$6.06224 \times 10^{-4}$	$1.21645 \times 10^{-5}$	$2.03221 \times 10^{-7}$	$2.90825 \times 10^{-9}$
	0.2	$9.51127 \times 10^{-3}$	$3.82944 \times 10^{-4}$	$1.28246 \times 10^{-5}$	$3.67705 \times 10^{-7}$
	0.3	$4.72281 \times 10^{-2}$	$2.8613 \times 10^{-3}$	$1.44062 \times 10^{-4}$	$6.20638 \times 10^{-6}$
	0.4	$1.46441 \times 10^{-1}$	$1.18662 \times 10^{-2}$	$7.98369 \times 10^{-4}$	$4.59368 \times 10^{-5}$
	0.5	$3.50848 \times 10^{-1}$	$3.56449 \times 10^{-2}$	$3.00433 \times 10^{-3}$	$2.16437 \times 10^{-4}$

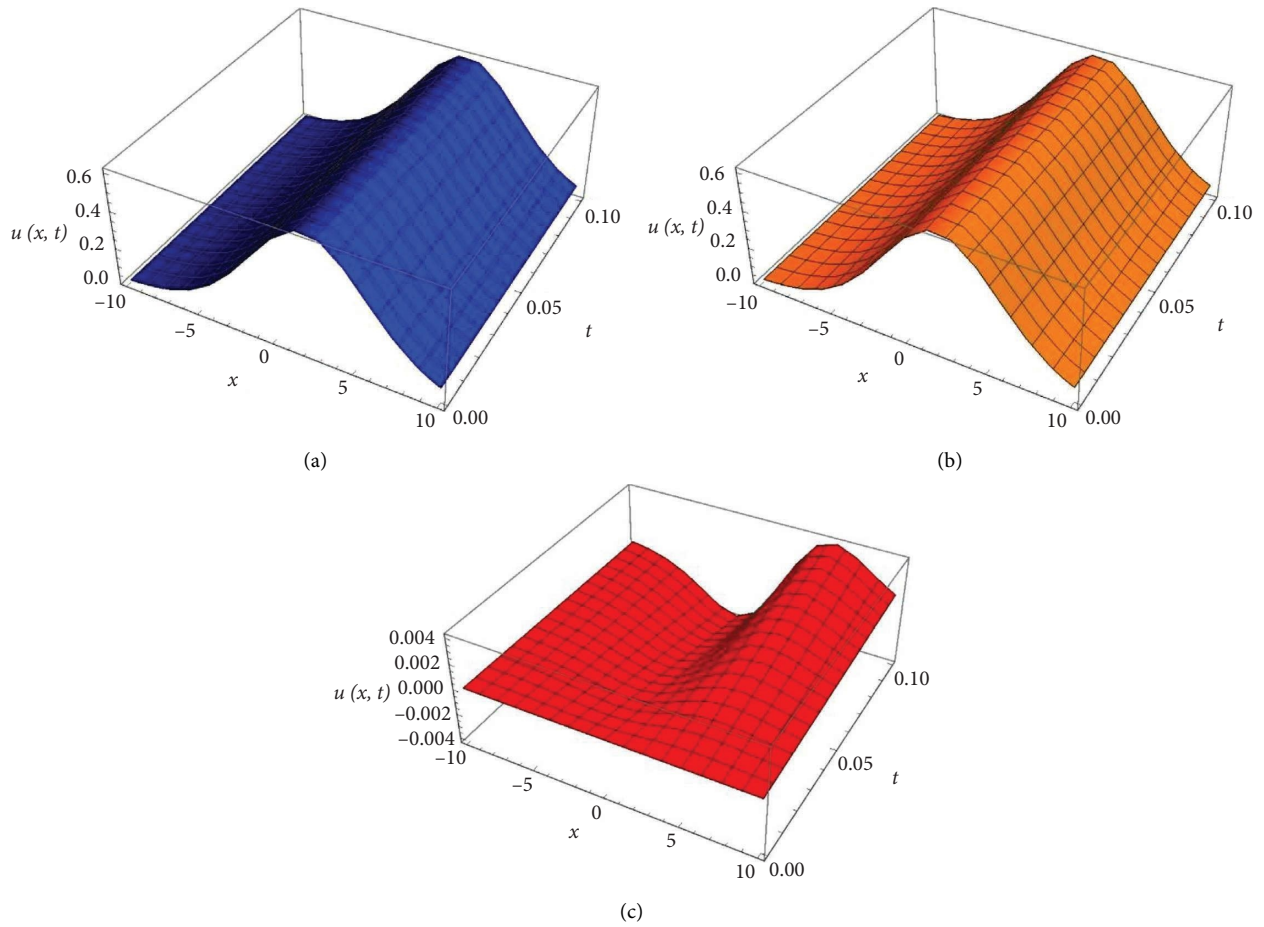


FIGURE 7: (a) 3D plot for the  $q$ -HATM solution, (b) surface of the exact solution, (c) approximated error solution surface, at  $\hbar = -1$ ,  $a = 4$ ,  $n = 1$ , and  $\alpha = 1$ .

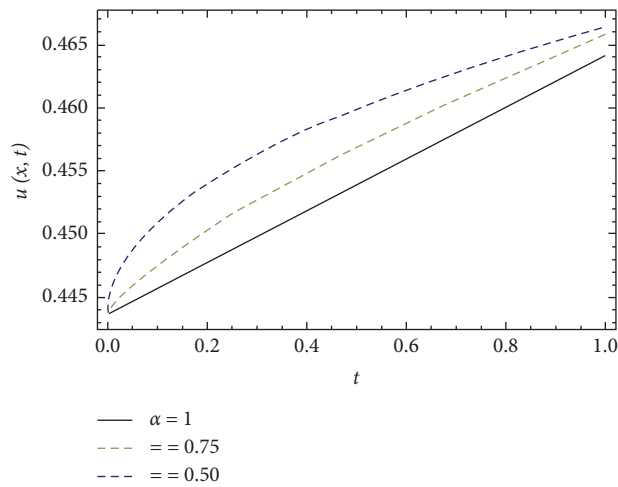


FIGURE 8:  $u(x, t)$  versus  $t$  for the contemplated Example 3 at  $\hbar = -1$ ,  $x = 5$ ,  $k = 2$ , and  $n = 1$  for distinct of  $\alpha$ .

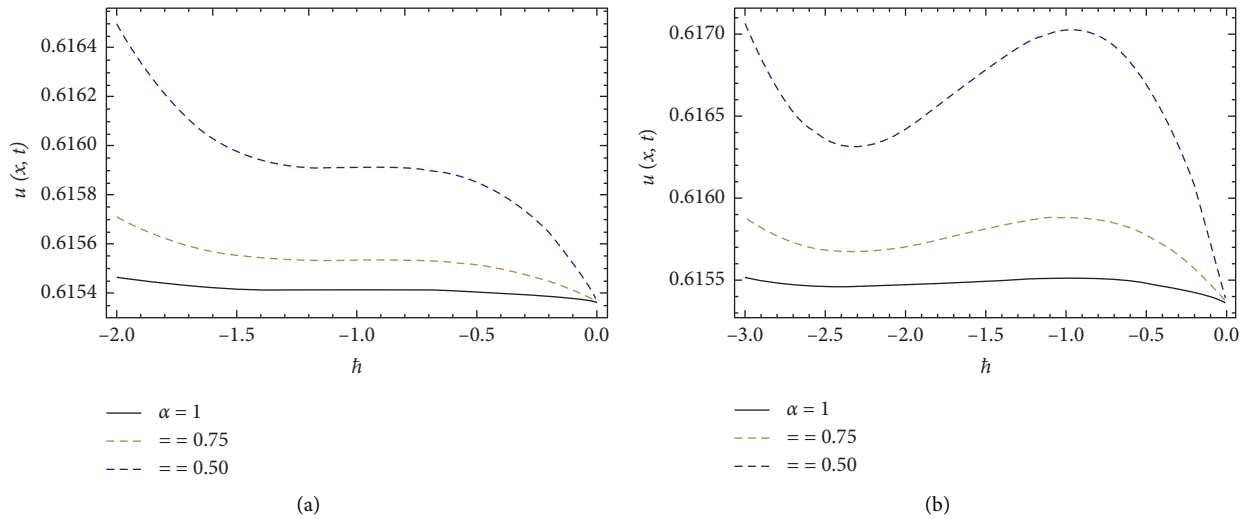


FIGURE 9:  $h$ -curve for acquired solution  $u(x, t)$  for Example 3 when (a)  $n = 1$  and (b)  $n = 2$  when  $x = 2.5, k = 2$ , and  $t = 0.01$  for distinct  $\alpha$ .

TABLE 3: Numerical study of the achieved results in terms of absolute error for Example 3 at  $h = -1, \alpha = 1$ , and  $n = 1$  and different values of  $x$  and  $t$ .

$x$	$t$	$u_{q\text{-HATM}}^{(2)}(x, t)$	$u_{q\text{-HATM}}^{(3)}(x, t)$
-5	0	0	0
	0.1	$2.11915 \times 10^{-3}$	$2.11916 \times 10^{-3}$
	0.2	$4.23833 \times 10^{-3}$	$4.23836 \times 10^{-3}$
	0.3	$6.35756 \times 10^{-3}$	$6.35768 \times 10^{-3}$
	0.4	$8.47686 \times 10^{-3}$	$8.47714 \times 10^{-3}$
	0.5	$1.05963 \times 10^{-2}$	$1.05968 \times 10^{-2}$
5	0	0	0
	0.1	$4.12712 \times 10^{-3}$	$4.12709 \times 10^{-3}$
	0.2	$8.25406 \times 10^{-3}$	$8.25384 \times 10^{-3}$
	0.3	$1.23807 \times 10^{-2}$	$1.23799 \times 10^{-2}$
	0.4	$1.65068 \times 10^{-2}$	$1.65050 \times 10^{-2}$
	0.5	$2.06322 \times 10^{-2}$	$2.06287 \times 10^{-2}$
10	0	0	0
	0.1	$1.47761 \times 10^{-3}$	$1.47762 \times 10^{-3}$
	0.2	$2.95525 \times 10^{-3}$	$2.95530 \times 10^{-3}$
	0.3	$4.43297 \times 10^{-3}$	$4.43312 \times 10^{-3}$
	0.4	$5.91079 \times 10^{-3}$	$5.91116 \times 10^{-3}$
	0.5	$7.38874 \times 10^{-3}$	$7.38947 \times 10^{-3}$

noticeably depends time and history behaviour. Moreover, the illustrated numerical simulations confirm the applicability as well as the accuracy of the considered solution procedure, and we proved that we can go close to the exact solution as we increase the number of iterations.

### 6. Conclusion

In the present work, the investigation of the time-fractional nonlinear fifth-order KdV equation is carried out using an analytical algorithm called  $q$ -HATM. We have taken three nonlinear problems to testify to the ability of the projected method to handle complex nonlinear problems. The results are highly pleasing and attest to the effectiveness of the strategy under consideration. The fractional operator considered in the present framework gives more degrees of

freedom and incorporates the nonlocal effect in the projected model. The innovative aspect of this approach is its straightforward process, which enables us to arrive at a solution quickly and identify a substantial region of convergence. The rate of convergence of the obtained series solution to the exact solution is accelerated with the help of optimal values of the convergence control parameter  $h$ . Presented numerical simulations guarantee the results with higher accuracy. Tables provide great satisfactory results when compared with the homotopy perturbation transform method (HPTM).

The defined homotopy may not produce the continuous family of terms in terms of the embedding parameter when using analytical procedures such as HPTM and other methods. By including a convergence control parameter in  $q$ -HATM, this constraint can be eliminated. The range of

auxiliary parameter  $\hbar$  that we get in the considered method is very small, we can achieve a better range of  $\hbar$  to accelerate the convergence of the obtained series solution by combining the presented method with suitable numerical techniques. As a future research direction, readers can use the hybrid methodologies merging with our projected scheme to achieve better consequences.

Finally, we claim that our proposed technique is incredibly dependable and can be applied to large study classifications relating to fractional-order nonlinear scientific methods, which aid us in better understanding the nonlinear compound phenomena in linked domains of innovation and science.

## Data Availability

No underlying data was collected or produced in this study.

## Conflicts of Interest

The authors declare that they have no conflicts of interest.

## References

- [1] G. F. B. Riemann, "Versucheinerallgemeinen auffassung der integration und differentiation," *Gesammelte Math. Werke Leipzig*, vol. 62, pp. 331–344, 1896.
- [2] I. Podlubny, *Fractional Differential Equations*, Academic Press, Cambridge, MA, USA, 1999.
- [3] J. Liouville, "Memoire sur quelques questions de geometrie et de mecanique, et sur un nouveau genre de calcul pour resoudreces questions," *Journal Ecole Polytechnique*, vol. 13, pp. 1–69, 1832.
- [4] K. S. Miller and B. Ross, *An Introduction to the Fractional Calculus and Fractional Differential Equations*, Wiley, Hoboken, NJ, USA, 1993.
- [5] M. Caputo, "Elasticita de dissipazione, zanichelli, bologna, italy,(links)," *SIAM journal on numerical analysis*, 1969.
- [6] D. Baleanu, G. C. Wu, and S. D. Zeng, "Chaos analysis and asymptotic stability of generalized Caputo fractional differential equations," *Chaos, Solitons & Fractals*, vol. 102, pp. 99–105, 2017.
- [7] P. Veerasha, D. G. Prakasha, and H. M. Baskonus, "New numerical surfaces to the mathematical model of cancer chemotherapy effect in Caputo fractional derivatives," *Chaos*, vol. 29, no. 1, Article ID 013119, 2019.
- [8] A. Qazza and R. Saadeh, "On the analytical solution of fractional SIR epidemic model," *Applied Computational Intelligence and Soft Computing*, vol. 2023, Article ID 6973734, 16 pages, 2023.
- [9] P. Veerasha and D. G. Prakasha, "A novel technique for (2+1)-dimensional time-fractional coupled Burgers equations," *Mathematics and Computers in Simulation*, vol. 166, pp. 324–345, 2019.
- [10] E. R. Pekünlü, Ö. Çakırlı, and E. Özetken, "Solar coronal heating by magnetosonic waves," *Monthly Notices of the Royal Astronomical Society*, vol. 326, no. 2, pp. 675–685, 2001.
- [11] D. Baleanu, Z. B. Guvenc, and J. A. T. Machado, *New Trends in Nanotechnology and Fractional Calculus Applications*, Springer, Berlin, Germany, 2010.
- [12] N. H. Sweilam, M. M. Abou Hasan, and D. Baleanu, "New studies for general fractional financial models of awareness and trial advertising decisions," *Chaos, Solitons & Fractals*, vol. 104, pp. 772–784, 2017.
- [13] R. Saadeh, A. Qazza, and K. Amawi, "A new approach using integral transform to solve cancer models," *Fractal and Fractional*, vol. 6, no. 9, p. 490, 2022.
- [14] D. Y. Kolotkov, D. I. Zavershinskii, and V. M. Nakariakov, "The solar corona as an active medium for magnetoacoustic waves," *Plasma Physics and Controlled Fusion*, vol. 63, no. 12, Article ID 124008, 2021.
- [15] P. Veerasha, D. G. Prakasha, A. H. Abdel-Aty, H. Singh, E. E. Mahmoud, and S. Kumar, "An efficient approach for fractional nonlinear chaotic model with Mittag-Leffler law," *Journal of King Saud University Science*, vol. 33, no. 2, Article ID 101347, 2021.
- [16] R. Hilfer, *Applications of Fractional Calculus in Physics*, World Scientific, Singapore, 2000.
- [17] M. A. Abdou, "An analytical method for space-time fractional nonlinear differential equations arising in plasma physics," *Journal of Ocean Engineering and Science*, vol. 2, no. 4, pp. 288–292, 2017.
- [18] M. Al-Smadi, O. Abu Arqub, and S. Momani, "Numerical computations of coupled fractional resonant Schrödinger equations arising in quantum mechanics under conformable fractional derivative sense," *Physica Scripta*, vol. 95, no. 7, Article ID 075218, 2020.
- [19] S. S. Chen, B. Tian, Y. Sun, and C. R. Zhang, "Generalized Darboux transformations, rogue waves, and modulation instability for the coherently coupled nonlinear Schrödinger equations in nonlinear optics," *Annalen der Physik*, vol. 531, no. 8, Article ID 1900011, 2019.
- [20] X. Sun, B. Zhang, Y. Li et al., "Tunable ultrafast nonlinear optical properties of graphene/MoS2 van der Waals heterostructures and their application in solid-state bulk lasers," *ACS Nano*, vol. 12, no. 11, pp. 11376–11385, 2018.
- [21] D. Kumar, C. Park, N. Tamanna, G. C. Paul, and M. S. Osman, "Dynamics of two-mode sawada-kotera equation: mathematical and graphical analysis of its dual-wave solutions," *Results In Physics*, vol. 19, Article ID 19103581, 2020.
- [22] M. Bilal, A. R. Seadawy, M. Younis, S. T. R. Rizvi, and H. Zahed, "Dispersive of propagation wave solutions to unidirectional shallow water wave Dullin–Gottwald–Holm system and modulation instability analysis," *Mathematical Methods in the Applied Sciences*, vol. 44, no. 5, pp. 4094–4104, 2021.
- [23] A. R. Seadawy, A. Ali, and W. A. Albarakati, "Analytical wave solutions of the (2+ 1)-dimensional first integro-differential Kadomtsev-Petviashvili hierarchy equation by using modified mathematical methods," *Results in Physics*, vol. 15, Article ID 102775, 2019.
- [24] R. A. Shahein and A. R. Seadawy, "Bifurcation analysis of KP and modified KP equations in an unmagnetized dust plasma with nonthermal distributed multi-temperatures ions," *Indian Journal of Physics*, vol. 93, no. 7, pp. 941–949, 2019.
- [25] I. Ali, A. R. Seadawy, S. T. R. Rizvi, M. Younis, and K. Ali, "Conserved quantities along with Painleve analysis and Optical solitons for the nonlinear dynamics of Heisenberg ferromagnetic spin chains model," *International Journal of Modern Physics B*, vol. 34, no. 30, Article ID 2050283, 2020.
- [26] K. K. Ali, M. A. Abd El Salam, E. M. H. Mohamed, B. Samet, S. Kumar, and M. S. Osman, "Numerical solution for generalized nonlinear fractional integro-differential equations with linear functional arguments using Chebyshev series," *Advances in Difference Equations*, vol. 2020, no. 1, pp. 494–523, 2020.

- [27] M. Ali Akbar, A. M. Wazwaz, F. Mahmud et al., "Dynamical behavior of solitons of the perturbed nonlinear Schrödinger equation and microtubules through the generalized Kudryashov scheme," *Results in Physics*, vol. 43, Article ID 106079, 2022.
- [28] Y. Saliou, S. Abbagari, A. Houwe et al., "W-shape bright and several other solutions to the  $(3+1)$ -dimensional nonlinear evolution equations," *Modern Physics Letters B*, vol. 35, no. 30, Article ID 2150468, 2021.
- [29] M. S. Osman, K. U. Tariq, A. Bekir et al., "Investigation of soliton solutions with different wave structures to the  $(2+1)$ -dimensional Heisenberg ferromagnetic spin chain equation," *Communications in Theoretical Physics*, vol. 72, no. 3, Article ID 035002, 2020.
- [30] S. Malik, H. Almusawa, S. Kumar, A. M. Wazwaz, and M. S. Osman, "A  $(2+1)$ -dimensional Kadomtsev–Petviashvili equation with competing dispersion effect: painlevé analysis, dynamical behavior and invariant solutions," *Results in Physics*, vol. 23, Article ID 104043, 2021.
- [31] I. Siddique, M. M. Jaradat, A. Zafar, K. Bukht Mehdi, and M. S. Osman, "Exact traveling wave solutions for two prolific conformable M-Fractional differential equations via three diverse approaches," *Results in Physics*, vol. 28, Article ID 104557, 2021.
- [32] D. J. Korteweg and G. de Vries, "XLI. On the change of form of long waves advancing in a rectangular canal, and on a new type of long stationary waves," *The London, Edinburgh, and Dublin Philosophical Magazine and Journal of Science*, vol. 39, no. 240, pp. 422–443, 1895.
- [33] J. Singh, D. Kumar, and S. Kumar, "A reliable algorithm for solving discontinued problems arising in nanotechnology," *Scientia Iranica*, vol. 20, no. 3, pp. 1059–1062, 2013.
- [34] R. Saadeh, O. Ala'yed, and A. Qazza, "Analytical solution of coupled Hirota–satsuma and KdV equations," *Fractal and Fractional*, vol. 6, no. 12, p. 694, 2022.
- [35] M. Almazmumy, F. A. Hendi, H. O. Bakodah, and H. Alzumi, "Recent modifications of adomian decomposition method for initial value problem in ordinary differential equations," *American Journal of Computational Mathematics*, vol. 02, no. 03, pp. 228–234, 2012.
- [36] H. O. Bakodah, "Modified adomian decomposition method for the generalized fifth order KdV equations," *American Journal of Computational Mathematics*, vol. 03, no. 01, pp. 53–58, 2013.
- [37] Y. Khan, "An effective modification of the Laplace decomposition method for nonlinear equations," *International Journal of Nonlinear Sciences and Numerical Stimulation*, vol. 10, no. 11-12, pp. 1373–1376, 2009.
- [38] A. Burqan, R. Saadeh, A. Qazza, and S. Momani, "ARA-residual power series method for solving partial fractional differential equations," *Alexandria Engineering Journal*, vol. 62, pp. 47–62, 2023, p.
- [39] A. Qazza, A. Burqan, R. Saadeh, and R. Khalil, "Applications on double ARA–sumudu transform in solving fractional partial differential equations," *Symmetry*, vol. 14, no. 9, p. 1817, 2022.
- [40] R. Hirota, "Exact solution of the Korteweg–de Vries equation for multiple collisions of solitons," *Physical Review Letters*, vol. 27, no. 18, pp. 1192–1194, 1971.
- [41] M. U. Ablowitz and P. A. Clarkson, "Solitons: nonlinear evolution equations and Inverse Scattering," *London Mathematical Society Lecture Note Series*, vol. 149, p. 516, 1991.
- [42] G. C. Wu and J. H. He, "Fractional calculus of variations in fractal spacetime," *Nonlin. Sci. Lett. A1*, vol. 3, pp. 281–287, 2010.
- [43] A. M. Wazwaz, "The extended tanh method for new soliton solutions for many forms of the fifth-order KdV equations," *Applied Mathematics and Computation*, vol. 184, no. 2, pp. 1002–1014, 2007.
- [44] S. Kumar, J. Singh, D. Kumar, and S. Kapoor, "New homotopy analysis transform algorithm to solve Volterra integral equation," *Ain Shams Engineering Journal*, vol. 5, no. 1, pp. 243–246, 2014.
- [45] S. Kumar and M. M. Rashidi, "New analytical method for gas dynamics equation arising in shock fronts," *Computer Physics Communications*, vol. 185, no. 7, pp. 1947–1954, 2014.
- [46] A. Yildirim, "An algorithm for solving the fractional nonlinear Schrödinger equation by means of the homotopy perturbation method," *International Journal of Nonlinear Sciences and Numerical Stimulation*, vol. 10, pp. 445–451, 2009.
- [47] L. A. Soltani and A. Shirzadi, "A new modification of the variational iteration method," *Computers & Mathematics with Applications*, vol. 59, no. 8, pp. 2528–2535, 2010.
- [48] D. D. Ganji, "The application of He's homotopy perturbation method to nonlinear equations arising in heat transfer," *Physics Letters A*, vol. 355, no. 4-5, pp. 337–341, 2006.
- [49] L. Xu, "He's homotopy perturbation method for a boundary layer equation in unbounded domain," *Computers & Mathematics with Applications*, vol. 54, no. 7–8, pp. 1067–1070, 2007.
- [50] G. Wang, A. H. Kara, K. Fakhar, J. Vega-Guzman, and A. Biswas, "Group analysis, exact solutions and conservation laws of a generalized fifth order KdV equation," *Chaos, Solitons & Fractals*, vol. 86, pp. 8–15, 2016.
- [51] C. Park, R. I. Nuruddeen, K. K. Ali, L. Muhammad, M. S. Osman, and D. Baleanu, "Novel hyperbolic and exponential ansatz methods to the fractional fifth-order Korteweg–de Vries equations," *Advances in Difference Equations*, vol. 2020, no. 1, pp. 627–712, 2020.
- [52] K. S. Nisar, O. A. Ilhan, S. T. Abdulazeez, J. Manafian, S. A. Mohammed, and M. S. Osman, "Novel multiple soliton solutions for some nonlinear PDEs via multiple Exp-function method," *Results in Physics*, vol. 21, Article ID 103769, 2021.
- [53] R. Saadeh, A. Qazza, and A. Burqan, "On the Double ARA–Sumudu transform and its applications," *Mathematics*, vol. 10, no. 15, p. 2581, 2022, p.
- [54] A. Qazza, A. Burqan, and R. Saadeh, "Application of ARA-residual power series method in solving systems of fractional differential equations," *Mathematical Problems in Engineering*, vol. 2022, Article ID 6939045, 17 pages, 2022.
- [55] A. Qazza, R. Saadeh, and E. Salah, "Solving fractional partial differential equations via a new scheme," *AIMS Mathematics*, vol. 8, no. 3, pp. 5318–5337, 2022.
- [56] A. Goswami, J. Singh, and D. Kumar, "Numerical simulation of fifth order KdV equations occurring in magneto-acoustic waves," *Ain Shams Engineering Journal*, vol. 9, no. 4, pp. 2265–2273, 2018.
- [57] T. Kawahara, "Oscillatory solitary waves in dispersive media," *Journal of the Physical Society of Japan*, vol. 33, no. 1, pp. 260–264, 1972.
- [58] J. Singh, D. Kumar, and R. Swroop, "Numerical solution of time-and space-fractional coupled Burgers' equations via homotopy algorithm," *Alexandria Engineering Journal*, vol. 55, no. 2, pp. 1753–1763, 2016.

- [59] S. J. Liao, *The proposed homotopy analysis technique for the solution of nonlinear problems*, Ph.D. Thesis, Shanghai Jiao Tong University, Shanghai, China, 1992.
- [60] L. Shijun, "Homotopy analysis method: a new analytic method for nonlinear problems," *Applied Mathematics and Mechanics*, vol. 19, no. 10, pp. 957–962, 1998.
- [61] P. Veerasha and D. G. Prakasha, "Solution for fractional generalized Zakharov equations with Mittag-Leffler function," *Results in Engineering*, vol. 5, pp. 100085–100112, 2020.
- [62] D. G. Prakasha, P. Veerasha, and J. Singh, "Fractional approach for equation describing the water transport in unsaturated porous media with Mittag-Leffler kernel," *Frontiers in Physiology*, vol. 7193 pages, 2019.
- [63] D. G. Prakasha, N. S. Malagi, and P. Veerasha, "New approach for fractional Schrödinger-Boussinesq equations with Mittag-Leffler kernel," *Mathematical Methods in the Applied Sciences*, vol. 43, no. 17, pp. 9654–9670, 2020.
- [64] A. A. Kilbas, H. M. Srivastava, and J. J. Trujillo, *Theory and Applications of Fractional Differential Equations*, Elsevier, Amsterdam, Netherlands, 2006.